

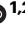



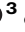
Arctic Sea Route access reshapes global shipping carbon emissions

Received: 9 January 2025

Accepted: 17 September 2025

Published online: 29 September 2025

 Check for updates

Pengjun Zhao ^{1,2}✉, Yunlin Li², Caixia Zhang ²✉, Tingting Kang², Zhangyuan He ², Guangyu Huang¹, Shiyi Zhang ², Xianghao Zhang², Yuanquan Xu ³ & Weiya Kong²

Climate-driven Arctic ice melt is opening the Arctic Sea Route (ASR), providing shorter paths for global trade while also raising critical environmental concerns. Here, we quantify the long-term carbon consequences of ASR access using a trade-integrated shipping emissions projection (TISEP) model that integrates trade scenarios, vessel routing, and climate policy pathways. Our results indicate that ASR use will increase global shipping emissions by 8.2% by 2100, with Arctic emissions rising from 0.22% to 2.72%. At the same time, environmental disparities in exposure to emissions will increase since North-east Asia, Northern Europe, and North America will experience particularly large increases in emissions due to rerouted shipping flows. We evaluate three mitigation strategies and find that two ongoing strategies, the 2023 IMO Strategy on Reduction of GHG Emissions from Ships and the Green Corridor strategy, are insufficient to achieve emission targets in the Arctic, but a net-zero strategy featuring stricter fuel standards and regionally phased rollout could fully eliminate ASR-related emissions. These findings highlight the urgent need for more prospective actions to reduce shipping emissions, protect the Arctic environment, and advance global environmental justice as Arctic navigability increases.

The Arctic is among the most climate-sensitive regions on Earth, with the retreat of sea ice accelerating as global temperatures rise^{1,2}. As this transformation continues, previously inaccessible Arctic passages—including the Northeast Passage, the Central Arctic Route, and the Northwest Passage—are becoming viable for commercial navigation^{3,4}. Collectively referred to here as the Arctic Sea Route (ASR), this emerging corridor can reduce the distance of voyages between Europe and Northeast Asia by as much as 40% and shorten transit times by as much as 30%^{5,6}. By 2030, access to the ASR is projected to increase trade volumes between these regions by 5% to 10%^{7,8} because of lower per-voyage fuel costs and improved network efficiency. These developments point to a gradual but significant shift in global maritime connectivity, with Arctic routes becoming

increasingly integrated into the evolving network of international shipping.

However, the environmental implications of expanded Arctic shipping remain a significant concern, particularly regarding long-term emissions trajectories and the spatial redistribution of carbon burdens^{9–12}. International shipping already accounts for nearly 3% of global anthropogenic CO₂ emissions^{13,14}. Although ASR access may reduce the amount of emissions per voyage through shorter routes, the overall climate benefit would be offset by the projected increases in total traffic, especially from carbon-intensive vessel classes such as oil, gas, and chemical tankers^{15–17}, which pose significant risks to ecologically vulnerable Arctic regions^{18–20}. The increases in total traffic will also create challenges to achieving the decarbonization targets set by

¹College of Urban and Environmental Sciences, Peking University, Beijing, China. ²School of Urban Planning and Design, Peking University Shenzhen Graduate School, Shenzhen, China. ³School of Environment and Resource, Guangxi Normal University, Guilin, China. ✉e-mail: pengjun.zhao@pku.edu.cn; zhangcaixia@pku.edu.cn

the International Maritime Organization (IMO) to reduce total annual greenhouse gas (GHG) emissions by at least 20% relative to 2008 levels by 2030, at least 70% by 2040, and reach net-zero emissions by around 2050^{12,21}. For the Arctic especially, the IMO has been promoting low-environment-impact initiatives, including the Polar Code²² and a scheduled ban on the use and carriage of heavy fuel oil (HFO) in Arctic waters²³. However, the effectiveness of these measures depends on enforcement, monitoring, and broad international compliance^{21,24}. Access to the ASR raises another issue in that the changes in global trade shipping routes may create environmental inequalities in emissions exposure between regions that experience increased trade flow and those that experience decreased trade flow.

While some earlier studies have examined the effects of access to the ASR on shipping emissions^{15,16,25,26}, significant gaps in the research remain. First, most of the existing literature focuses on the local environmental impacts of access to the ASR in the Arctic region^{18,19,23} while the impacts on global shipping emissions have received little attention. In particular, the geographic redistribution of carbon burdens and the resulting environmental inequalities in exposure to emissions across regions have not been sufficiently addressed^{16,27}. Second, a practical prospective scenario for achieving zero emissions in the Arctic is lacking^{21,28}. Third, there is a shortage of comprehensive prediction models that integrate global trade forecasts, shipping route decisions, and alternative fuel scenarios, for most current models focus either on routing efficiency^{21,26,29} or global trade projections^{27,30} in isolation. There is, therefore, a pressing need for an integrated, forward-looking framework that links trade intensity, routing dynamics, and international climate goals.

Here, we develop a trade-integrated shipping emissions projection (TISEP) model that integrates future trade scenarios, vessel routing, and climate policy pathways into a unified framework. The model quantifies the overall increase in global shipping carbon emissions attributable to the opening of the ASR while also capturing the spatial redistribution of emissions, in particular, the emergence of additional hotspots in ecologically vulnerable Arctic waters and along major global shipping corridors. It accounts for Arctic-specific operational constraints such as seasonal and interannual sea ice variability requiring ice-class vessels and regulatory measures such as the IMO's ban on HFO in Arctic waters. These features enable the model to realistically simulate both climate- and policy-driven changes in shipping routes and emissions. To capture the uncertainty in future trade trajectories, we construct two contrasting scenarios: an optimistic trade scenario (OTS) driven by macroeconomic growth and cost-based integration (e.g., Gross Domestic Product (GDP), distance, and transport cost) and a pessimistic trade scenario (PTS) reflecting rising geopolitical risks and trade protectionism. These scenarios are aligned with the shared socioeconomic pathways (SSPs) used in Intergovernmental Panel on Climate Change (IPCC) assessments and calibrated with more than 6.49 billion Automatic Identification System (AIS) signals and empirically derived trade elasticities (see Methods). By simulating global vessel flows and the associated emissions across these trade and policy futures, the TISEP enables a spatially resolved, policy-relevant assessment of how access to the ASR will reshape the scale and distribution of maritime carbon emissions. This assessment highlights not only the implications for overall decarbonization but also the emerging equity risks embedded in the evolving structure of global shipping networks.

Leveraging this framework, we examine how three decarbonization strategies shape future emissions trajectories and spatial outcomes under various trade and routing scenarios. Two of these strategies, the 2023 IMO Strategy on Reduction of GHG Emissions from Ships (IMO 2023 strategy)¹² and the Green Corridor strategy^{31,32} are supported by international efforts involving the IMO. The IMO 2023 strategy reflects the organization's revised GHG reduction targets and assumes a sector-wide shift toward low- and zero-carbon fuels

through gradual compliance mechanisms. The Green Corridor strategy builds on this approach by accelerating green fuel deployment along maritime routes selected for their geopolitical or ecological significance. The third strategy, Net-Zero, introduces a structurally distinct decarbonization pathway anchored in two core features: stricter fuel standards and a regionally phased rollout. The first feature centers on a tank-to-wake emissions boundary, requiring zero emissions at the point of combustion, and marks a fundamental departure from the well-to-wake accounting in the IMO 2023 and Green Corridor strategies^{32,33}, which credit upstream mitigation but allow significant emissions at sea. To meet this stricter criterion, the Net-Zero strategy prioritizes the deployment of truly zero-emission energy carriers—specifically, electricity, hydrogen, and nuclear propulsion^{34–36}. The second feature involves spatially staged implementation, beginning in the Arctic, where ecological sensitivity is greatest, by 2040 and extending globally after 2050. This phased rollout enables the sector to reach full operational decarbonization by 2100. The projections of the TISEP model show that neither the IMO 2023 strategy nor the Green Corridor strategy would fully eliminate Arctic emissions by the end of the century. By contrast, the Net-Zero strategy, through a combination of fuel strictness and geographic prioritization, would not only achieve zero emissions in the Arctic but also help mitigate global environmental inequalities in shipping-related pollution exposure.

Results

The impacts of opening the ASR on the flow of global shipping

The opening of the ASR will reshape global maritime trade, positioning the Bering Strait as a critical chokepoint. Currently, dense sea ice limits Arctic voyages to less than 2000 while traffic is concentrated in the Suez Canal, the Panama Canal, and the Strait of Malacca (Fig. 1a). The retreat of the ice and the growth of trade will alter this pattern. Thus, by 2050, ASR voyages, mainly through the Northeast Passage, are projected to reach 12,218 under the PTS and 23,205 under the OTS (Fig. 1b). After 2070, improved ice conditions are expected to trigger a sharp increase in the flow of vessels through the Northwest Passage and Central Arctic Route. By 2100, the Arctic is expected to support year-round navigation for all major vessel types, allowing the ASR to handle 2.25% of global traffic (569,214 voyages) under the OTS or 2.07% (180,608 voyages) under the PTS, surpassing the Suez Canal (OTS: 163,339) and Panama Canal (OTS: 331,435) (Fig. 1c, d). Compared with the counterfactual scenario without access to the ASR (Fig. 1e, f), the flow of cargo through the Bering Strait would increase by 94.2% to 99.8% under the OTS, and traffic through the Suez and Panama Canals would decline by up to 5.1% and 3.6%, respectively (Fig. 1g), reflecting the cost-driven rerouting that will divert shipping flows toward the Arctic.

The ASR will drive a structural shift in global shipping patterns, with impacts varying by vessel type and trade scenario. Oil and gas tankers will dominate Arctic traffic, accounting for 67.52% of ASR voyages by 2100 under the OTS or 58.38% under the PTS (Supplementary Table 1). As East Asian demand grows, Arctic rerouting will become increasingly prominent along the energy corridors connecting Japan and South Korea with European partners, with ASR usage reaching 43% to 56% (Supplementary Fig. 1). Bulk and chemical carriers, initially concentrated along southbound routes, will shift progressively northward, with the ASR emerging as a key conduit for Russian exports (Supplementary Figs. 1 and 2). By contrast, container vessels—being constrained by hub-and-spoke infrastructure—will undergo limited rerouting except along select links between East Asia and Northern Europe. These patterns are highly sensitive to trade intensity. Under the PTS, ASR voyages on major energy routes such as Vietnam–Norway, Vietnam–Denmark, and South Korea–Germany will decline by about 75% relative to the OTS (Supplementary Fig. 3). A differential analysis (OTS minus PTS) shows that oil exports from Vietnam and South Korea–Germany gas routes will increase the most,

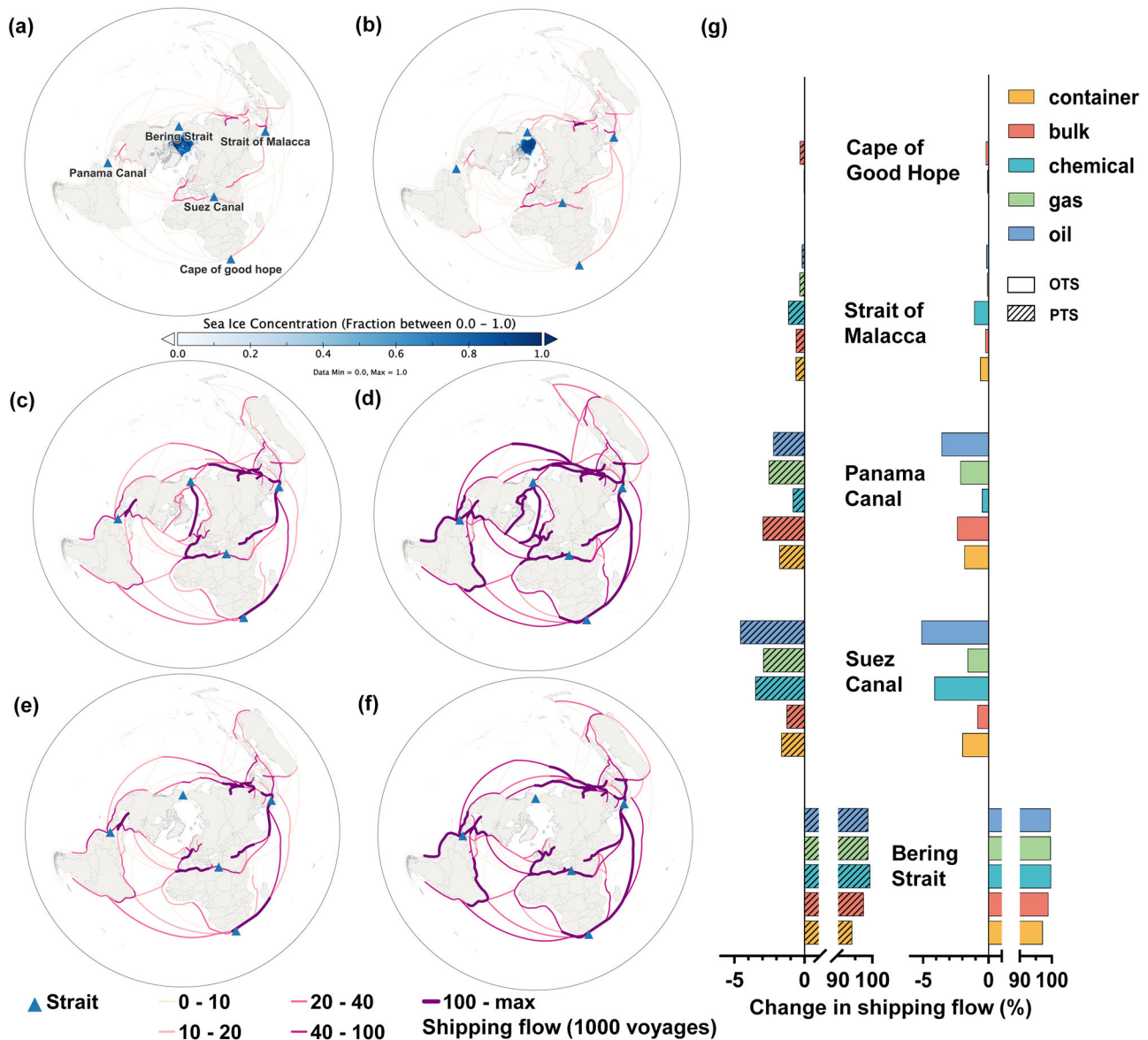


Fig. 1 | Global shipping flows with and without Arctic Sea Route (ASR) access, 2022–2100, under the optimistic trade scenario (OTS) and pessimistic trade scenario (PTS). a Global shipping flows in 2022 overlaid with Arctic sea ice concentration; **b** projected shipping flows in 2050 under the OTS, with partial Arctic sea ice retreat; **c** projected shipping flows in 2100 under PTS; **d** projected shipping

flows in 2100 under the OTS; **e** counterfactual scenario: shipping flows in 2100 under the PTS assuming no ASR access; **f** counterfactual scenario: shipping flows in 2100 under the OTS assuming no ASR access; **g** impact of ASR access on shipping flows in 2100 at key global chokepoints (the Bering Strait, the Suez Canal, the Panama Canal, the Strait of Malacca, and the Cape of Good Hope).

with more than 5000 additional ASR voyages by 2100 (Supplementary Fig. 4). Despite these increases, the overall reliance on the ASR will remain moderate (<50% voyages) for oil and gas transport, thus underscoring the role of the ASR as a region- and cargo-specific corridor within a globally diversified network. These results indicate that the spatial redistribution of global shipping flows will be uneven, particularly for high-emission vessel classes rerouting toward the Arctic, and raise pressing concerns about the emerging role of the Arctic in global maritime carbon emissions.

Shipping carbon emissions projections under the business-as-usual scenario

The Arctic is emerging as a critical frontier for maritime carbon emissions under the business-as-usual (BAU) scenario. With fuel structures unchanged and trade volumes rising, the opening of the ASR is projected to drive a substantial increase in shipping carbon emissions across the North Polar Region (Fig. 2a; Supplementary

Figs. 5, 6). According to the TISEP model, emissions are expected to rise from a minimal baseline of 1.01 megatonnes (Mt) carbon dioxide equivalent (CO_{2eq}) in 2022 to 117.61 Mt under the OTS and 36.25 Mt under the PTS by 2100, with the Central Arctic Route contributing 58.28%, the Northeast Passage 17.25%, and the Northwest Passage 24.47%. Consequently, the ASR is poised to become one of the five most carbon-intensive shipping corridors globally, with its share of global maritime emissions rising from 0.22% to 2.72% under the OTS or 1.01% under the PTS. This escalation—largely occurring after 2050—will be driven primarily by increasing traffic from gas, oil, and chemical tankers, which together account for 87.37% of ASR emissions under the OTS and 81.05% under the PTS. Although access to the ASR will shorten voyages and reduce per-trip emissions, these gains will be offset by a sharp increase in overall traffic across all vessel classes, including bulk, container, oil, chemical, and gas carriers.

At the global scale, maritime emissions are also projected to surge dramatically this century, with the Northern Hemisphere accounting

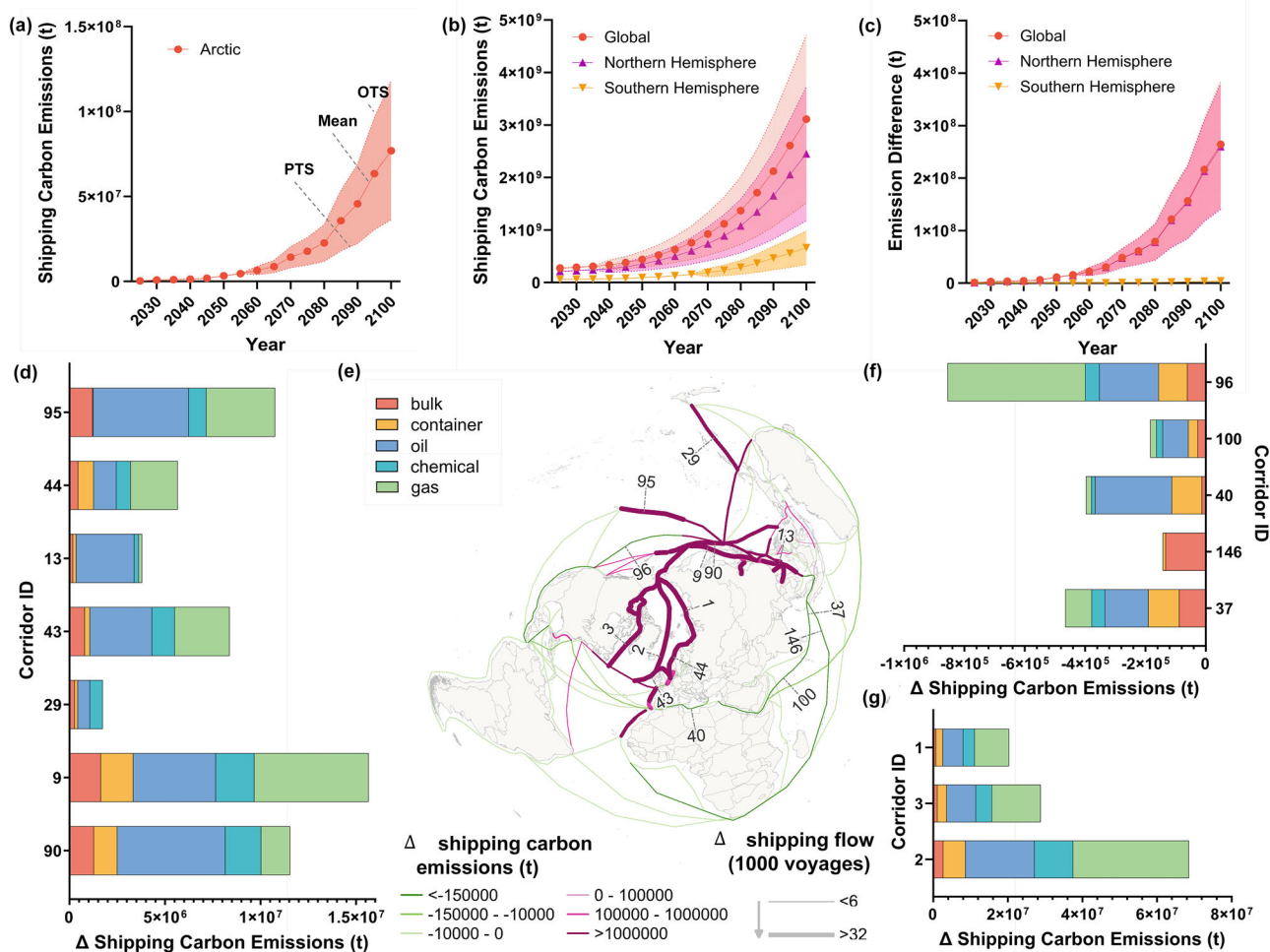


Fig. 2 | Evolution and spatial redistribution of global shipping carbon emissions resulting from Arctic Sea Route (ASR) access from 2025 to 2100 under the business-as-usual trade scenario. **a** Projected Arctic shipping emissions with ASR access, disaggregated by vessel type (bulk, container, oil, chemical, and gas carriers); **b** global and hemispheric trajectories of shipping carbon emissions with ASR access over time; **c** net increases in global and hemispheric shipping emissions attributable to ASR access by 2100 relative to a no-ASR counterfactual; **d** Corridors with the largest net increases in shipping carbon emissions by 2100 attributable to ASR access (stacked by vessel type); **e** Spatial distribution of net changes in shipping carbon emissions across major shipping routes by 2100 attributable to ASR access; **f** Corridors exhibiting net decreases in shipping carbon emissions by 2100

attributable to ASR access (stacked by vessel type); **g** Arctic major routes with substantial net increases in shipping carbon emissions by 2100 attributable to ASR access (stacked by vessel type). Key routes and chokepoints referenced in panels (d–g) include the Arctic Northeast Passage (1), the Central Arctic Route (2), the Arctic Northwest Passage (3), the Tsugaru Strait (9), the Taiwan Strait (13), the Luzon Strait (90), the Coral Sea (northeastern Australia) (29), the Malacca Strait (37), the Suez Canal (40), the United States–United Kingdom (US–UK) corridor (43), the Oslo–Rotterdam corridor (44), the North Pacific Transoceanic corridor (95), the North Pacific corridor (96), the South Arabian Sea corridor (100), and the Indian Ocean Transoceanic corridor (146).

for a disproportionate share of the increase. Under the OTS (Fig. 2b), emissions are projected to rise from 217.20 Mt CO_{2eq} in 2022 to 4.71 gigatonnes (Gt) CO_{2eq} by 2100, a 22-fold increase (sevenfold under the PTS). The Northern Hemisphere consistently contributes ~80% of total maritime emissions while the Southern Hemisphere follows a more moderate trajectory. The opening of the ASR will reinforce this hemispheric disparity structurally by redirecting traffic toward higher-emitting northern corridors. Compared with a counterfactual without use of the ASR, global emissions will increase by 384.29 Mt CO_{2eq} under the OTS by 2100 (Fig. 2c), an 8.2% rise (+143.67 Mt; +9.5% under the PTS). These findings underscore the substantial net emissions impact of the ASR, with nearly all of the additional carbon burden concentrated in the Northern Hemisphere (98.67% under the OTS; 97.82% under the PTS).

Spatially, Arctic carbon emissions are highly uneven, being concentrated in a few high-impact sea areas (Fig. 2d–g, Supplementary

Fig. 7). Up to 2070, most Arctic transits—and associated emissions—will occur along the Northeast Passage, particularly through the Kara Sea (2070: 4.07 Mt under the OTS; 1.62 Mt under the PTS) and East Siberian Sea (3.09 Mt under the OTS; 1.23 Mt under the PTS), where navigability is relatively favorable. Emissions will also rise sharply in the Laptev and Chukchi Seas, in both cases exceeding 1.2 Mt under the OTS and 0.4 Mt under the PTS. After 2070, as sea ice retreats further, shipping traffic will shift markedly toward the Central Arctic Ocean and the Canadian Arctic Archipelago, driven by shorter routing distances and lower operational costs. By 2100, this transition will intensify carbon-intensive activity in previously inaccessible waters, in particular, the Lincoln Sea (31.65 Mt under the OTS; 9.62 Mt under the PTS), Baffin Bay (18.32 Mt under the OTS; 5.68 Mt under the PTS), and Norwegian Sea (10.71 Mt under the OTS; 3.26 Mt under the PTS), broadening the spatial footprint of Arctic shipping emissions (Fig. 2e). These shifts will both diversify the geographic distribution of maritime traffic and

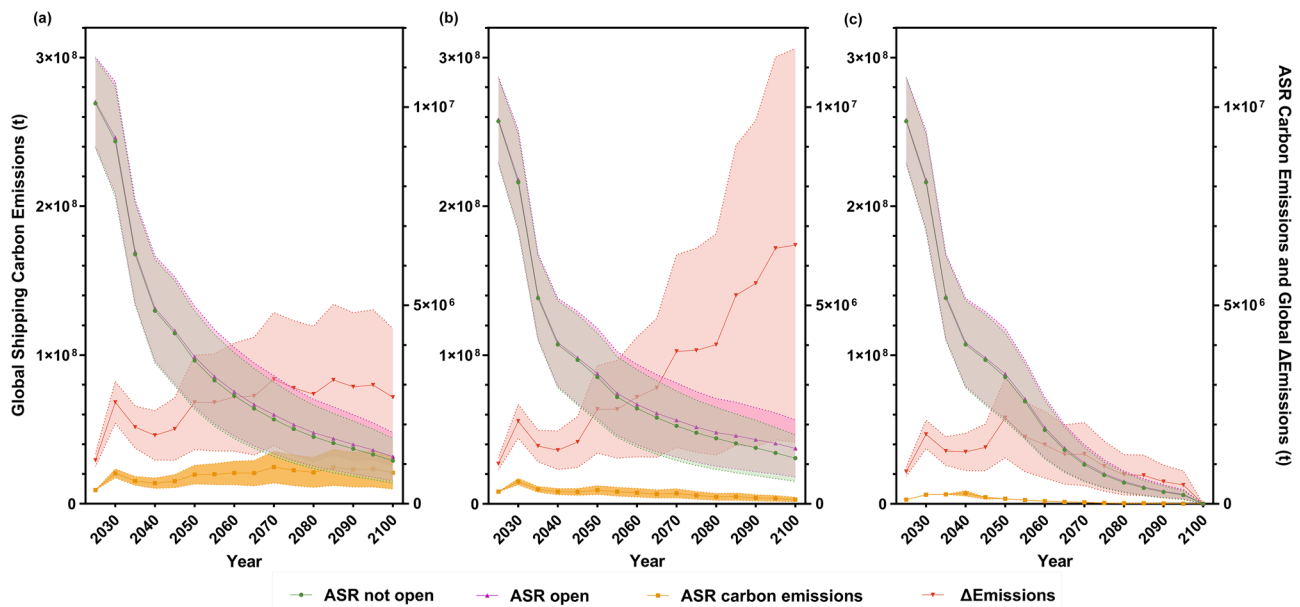


Fig. 3 | Temporal impacts of the opening of the Arctic Sea Route (ASR) on global shipping carbon emissions under three decarbonization strategies from 2025 to 2100. Each panel displays projected global shipping carbon emissions and associated ASR-induced emission changes under: **a** the IMO 2023 Strategy, **b** the Green Corridor Strategy, and **c** the Net-Zero Strategy. For each strategy, the solid green line represents global emissions without ASR access while the solid pink line

shows emissions with ASR access. The orange line reflects emissions occurring specifically along ASR corridors. The red line indicates the net increase in global emissions attributable to ASR access ($\Delta\text{Emissions} = \text{with ASR} - \text{without ASR}$). The upper and lower bounds of each shaded band represent emissions under the Optimistic Trade Scenario (OTS) and the Pessimistic Trade Scenario (PTS), respectively.

concentrate emissions in ecologically sensitive and historically low-impact regions, reinforcing the need for region-specific mitigation and monitoring strategies.

Beyond the Arctic, ASR-induced rerouting will produce stark geographic disparities in global maritime emissions with the intensification of regional hotspots in East Asia, Northern Europe, and North America (Fig. 2d). In the Northwest Pacific, increases of 30–50 Mt $\text{CO}_{2\text{eq}}$ are projected along key chokepoints, including the Tsugaru, Luzon, and Taiwan Straits (corridor IDs 9, 90, and 13), under the OTS, representing two- to five-fold surges in emissions relative to the no-ASR baselines. These surges will be driven primarily by oil, gas, and chemical tankers, with combined emissions reaching 43.4–85.8 Mt annually near China, Japan, and South Korea across the South China Sea, East China Sea, and Sea of Japan. Northern Europe will also experience substantial growth, most prominently along the Oslo–Rotterdam corridor (ID 44), with emissions increasing more than sixfold, from 5.30 Mt to 39.37 Mt. A similar pattern is expected along the United States–United Kingdom (US–UK) corridor (ID 43), with emissions increasing by 25.38 Mt $\text{CO}_{2\text{eq}}$ (from 10.99 Mt to 36.37 Mt). Thus, the North Sea will be among the maritime regions most impacted. By contrast, equatorial chokepoints such as the Malacca Strait (ID 37), the Suez Canal, and the Panama Canal will experience slight reductions (0.49–0.70 Mt per segment) because of the diversion of cargo away from these routes (Fig. 2f). Most Southern Hemisphere corridors will experience modest declines, with the notable exception of Australia’s northeastern Coral Sea (ID 29), where emissions are projected to rise from 1.74 Mt to 6.06 Mt because of the increased trans-Pacific traffic.

Shipping decarbonization strategies

In light of these trends, we evaluate how alternative decarbonization strategies may alter Arctic and global shipping carbon emissions. Specifically, we assess the three strategy scenarios described earlier: the IMO 2023 strategy, a Green Corridor strategy, and the Net-Zero strategy introduced in this study (detailed in the Methods section). The

long-term mitigation effectiveness of these scenarios differs substantially (Fig. 3; Supplementary Figs. 8 and 9). Under the BAU baseline, Arctic emissions would rise steeply, as noted. The IMO 2023 strategy (Fig. 3a) would moderate but not reverse this trend, with emissions peaking at -1.32 Mt $\text{CO}_{2\text{eq}}$ by 2070. The Green Corridor strategy would perform better, with emissions peaking earlier, in 2030, at -0.63 Mt before declining. Only the Net-Zero strategy delivers near-linear reductions, reaching zero emissions by 2100 with >90% cumulative abatement relative to IMO 2023 strategy. The persistence of these differences even under the PTS underscores the primacy of policy ambition over trade volume in shaping Arctic climate outcomes.

While the long-term trajectories of these strategies differ markedly, their structural robustness remains a key concern. To assess the resilience of decarbonization policies to structural changes in the shipping network, we compare projected global emissions trajectories with and without access to the ASR. Even in the absence of access, residual emissions would remain considerable under both the IMO 2023 strategy (43.97 Mt $\text{CO}_{2\text{eq}}$) and the Green Corridor strategy (46.46 Mt $\text{CO}_{2\text{eq}}$) by 2100, indicating incomplete decarbonization (Fig. 3a, b). By contrast, the Net-Zero strategy would sustain near-zero emissions throughout the second half of the century regardless of access to the ASR (Fig. 3c). This divergence highlights the key insight that effective mitigation depends not only on policy ambition but also on the capacity to absorb structural shocks such as the opening of major routes. Under the IMO 2023 and Green Corridor strategies, emissions persist because the traffic and the associated carbon shift to other high-emission routes. Only the Net-Zero strategy fully addresses this systemic vulnerability by decarbonizing the entire maritime network independent of future routing configurations.

To quantify the marginal impact of the ASR, we calculate the net difference in global emissions between these strategies with and without access to it. Under the IMO 2023 strategy, the ASR will contribute an additional 3.91 Mt $\text{CO}_{2\text{eq}}$ by 2100—a 9% increase over the baseline without the ASR. Somewhat counterintuitively, the Green Corridor strategy performs worse, with use of the ASR leading to

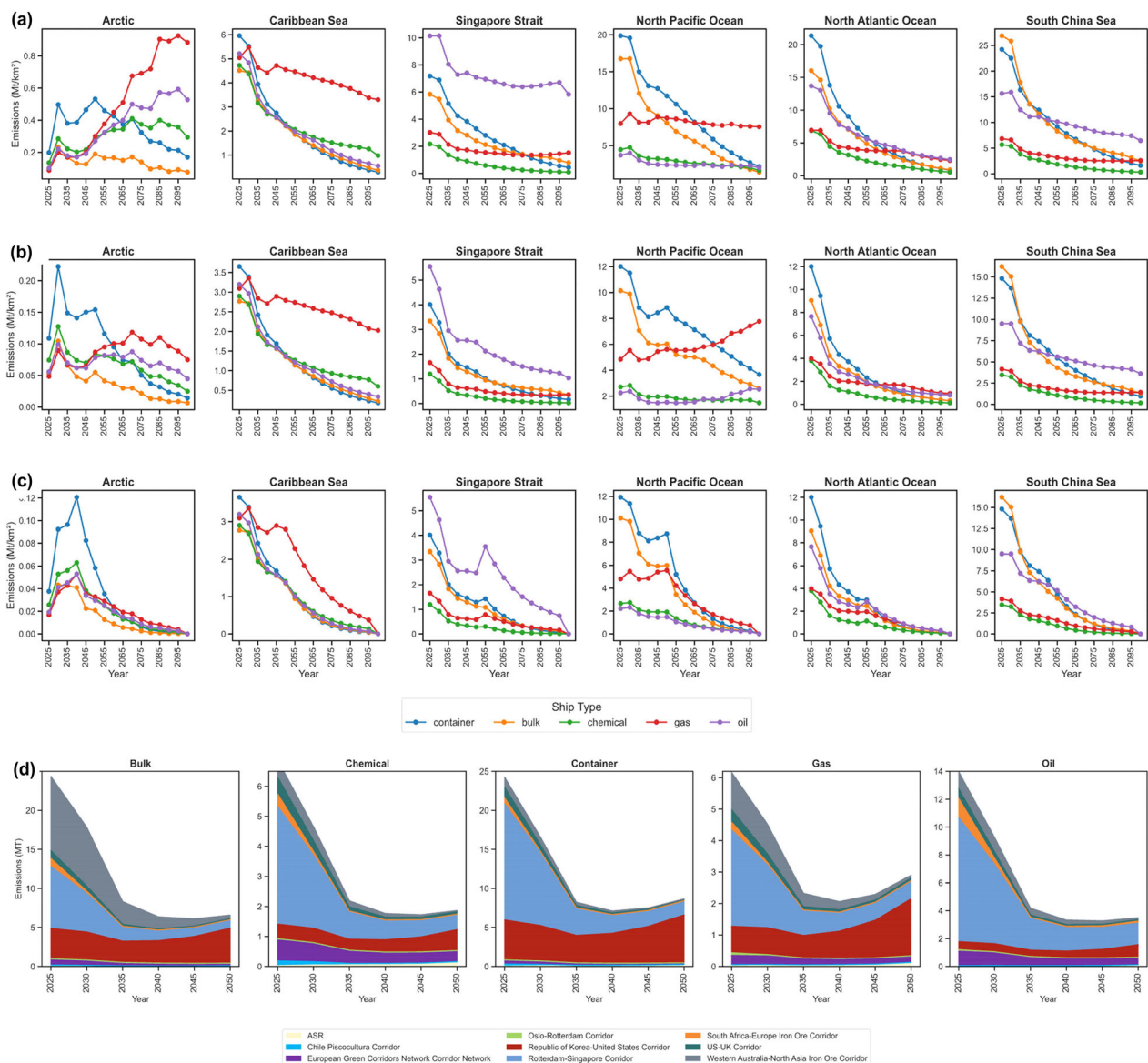


Fig. 4 | Projected regional shipping carbon emissions by ship type under three decarbonization strategies. Spatial projections of emission intensity ($\text{Mt CO}_{2\text{eq}} \text{ km}^{-2}$) from 2025 to 2100 under **a** the IMO 2023 Strategy, **b** the Green Corridor Strategy, and **c** the Net-Zero Strategy across six major sea regions, namely, the Arctic, the Caribbean Sea, the Singapore Strait, the North Pacific Ocean, the North Atlantic Ocean, and the South China Sea. Each subplot shows emissions disaggregated by ship type: container, bulk, chemical, gas, and oil. **d** Sectoral distribution of projected carbon emissions along key green shipping corridors from 2025 to 2050.

Atlantic Ocean, and the South China Sea. Each subplot shows emissions disaggregated by ship type: container, bulk, chemical, gas, and oil. **d** Sectoral distribution of projected carbon emissions along key green shipping corridors from 2025 to 2050.

10.03 $\text{Mt CO}_{2\text{eq}}$ in added emissions (+22%) despite the stronger regional mitigation measures. The performance of this strategy reflects a rebound effect, with targeted decarbonization efforts in specific corridors driving traffic—and emissions—to less-regulated parts of the network. The Net-Zero strategy, however, eliminates this marginal impact entirely. The contrast among these strategies makes clear the critical importance of system-wide decarbonization efforts that neutralize both geographic and network-induced rebound effects.

Spatially, under the IMO 2023 strategy (Fig. 4a), emissions would intensify most sharply in the Arctic, especially those from gas and oil carriers, rising from $<0.05 \text{ Mt km}^{-2}$ in 2025 to $>0.87 \text{ Mt km}^{-2}$ by 2100, and traditional chokepoints such as the Singapore Strait and North Pacific Ocean would experience reductions of more than 50%. The Green Corridor strategy (Fig. 4b) would reduce emissions in most targeted regions (e.g., those of container ships in the Singapore Strait from 6.65 to 0.24 Mt km^{-2}) but would fail to control growth in

the Arctic, where mitigation gaps would persist. Under the Net-Zero strategy (Fig. 4c), all ship types would converge to near-zero emissions across all regions, including the Arctic, despite traffic growth—an outcome that demonstrates the robustness of full-fleet decarbonization. These findings likewise reflect the emergence of the Arctic as the primary residual emissions hotspot under partial mitigation strategies.

Further structural contrasts emerge across major green shipping corridors (Fig. 4d, Supplementary Fig. 10). Initially, the ASR would be dominated by container and chemical tankers, the emissions from which would peak before 2035 and then decline. The Rotterdam-Singapore corridor would remain container-dominant while the emission shares from the Republic of Korea-United States and ASR corridors would rise significantly, from 14.43% to 59.69% and from near zero to 0.02%, respectively. These shifts indicate that the emerging trade corridors are expanding faster than policy enforcement and

expose latent vulnerabilities that would persist even under the partially mitigated decarbonization regimes.

Discussion

The results of our TISEP model indicate that the opening of the ASR will not only reshape regional shipping patterns but also amplify global carbon emissions and exacerbate environmental inequalities. Under the BAU scenario, Arctic maritime emissions are projected to surge from 1.00 Mt CO_{2eq} in 2022 to 117.61 Mt by 2100 in the high trade case, driven primarily by a sharp increase in traffic from oil, gas, and chemical tankers³⁷, which together would account for more than 80% of ASR emissions. The contribution of the ASR to global maritime emissions would rise more than twelvefold, from 0.22% to 2.72%, making this route one of the five most carbon-intensive corridors worldwide. Spatially, emissions would intensify in newly navigable but ecologically vulnerable waters^{38,39}, with hotspots such as the Lincoln Sea (31.65 Mt) and Baffin Bay (18.32 Mt), which were previously near-zero emission zones, emerging as critical carbon concentration zones. This transformation risks accelerating Arctic warming, disrupting albedo effects and permafrost stability, which could release significant methane stores and exacerbate global climate feedbacks. Although access to the ASR reduces voyage distances, these efficiency gains will be overwhelmed by the scale of increased traffic growth. These findings underscore the Arctic's role as an emerging emissions frontier, challenging global decarbonization efforts like the Paris Agreement's 1.5 °C target and highlighting the need for region-specific mitigation to protect its critical ecological functions.

Beyond the Arctic, ASR-induced rerouting will trigger pronounced spatial shifts in global shipping emissions that will deepen regional disparities in environmental exposure. High-emission traffic will be redirected away from traditional chokepoints such as the Suez and Panama Canals toward high-latitude corridors, resulting in substantial emission increases across Northeast Asia, Northern Europe, and North America. For example, annual emissions along the Oslo–Rotterdam corridor will increase from 5.30 Mt to 39.37 Mt, and those along the US–UK corridor will increase by 25.38 Mt, transforming the North Sea into one of the world's most impacted maritime regions. In the Northwest Pacific, emissions through the Tsugaru, Luzon, and Taiwan Straits will increase by 30–50 Mt CO_{2eq} primarily because of the rerouting of oil, gas, and chemical tankers serving East Asian economies. These shifts, driven by carbon-intensive tankers, could increase ocean acidification risks in northern corridors, threatening marine ecosystems critical for global fisheries and biodiversity. By contrast, equatorial corridors such as the Malacca Strait and the Suez Canal will experience marginal declines in emissions in another example of the hemispheric redistribution of maritime carbon burdens. These asymmetric outcomes reflect a critical inequity: while exporting nations stand to benefit economically from Arctic access, emissions will increasingly be offshored to ecologically sensitive and under-regulated transit zones, disproportionately impacting Arctic indigenous communities reliant on marine resources for cultural and economic survival.

Our evaluation of decarbonization strategies also indicates that current international efforts fall short of mitigating ASR-induced emissions, particularly in the Arctic. Under the IMO 2023 strategy, Arctic shipping emissions would peak at -1.32 Mt CO_{2eq} by 2070 while the Green Corridor strategy would reduce this peak only to -0.63 Mt, with emissions persisting through 2100. Counterintuitively, access to the ASR under the Green Corridor scenario would increase global emissions by 22% relative to the situation without access because of the rebound effect in non-regulated regions. By contrast, our proposed Net-Zero strategy would nearly eliminate Arctic shipping emissions by 2100, delivering >90% cumulative abatement compared with the IMO baseline and neutralizing the global marginal impact of the ASR. This success stems from its systemic approach, addressing

network-wide traffic shifts and preventing residual emissions that could trigger ecological tipping points, such as accelerated ice loss or permafrost thaw. These results underscore the necessity of system-wide fuel transitions and show that partial or geographically constrained policies cannot safeguard the Arctic from long-term emissions growth or mitigate global environmental inequity, particularly when well-to-wake accounting allows tailpipe emissions that harm Arctic air quality and ice integrity.

The structural ambition and spatial targeting of the Net-Zero strategy account for its effectiveness. Unlike existing frameworks that rely on incremental fuel substitution or route-specific mitigation, Net-Zero mandates a universal transition to zero-emission energy carriers, including green hydrogen, electricity, and nuclear propulsion^{34–36}, with an Arctic-prioritized rollout beginning in 2040. This early deployment in high-latitude regions would address the heightened climate sensitivity in these regions and prevent emissions from leaking into ecologically fragile waters. By 2050, the strategy would expand globally, enabling complete fleet-wide decarbonization by the century's end. However, its implementation faces challenges, including high upfront costs for hydrogen and electrification infrastructure, as well as geopolitical barriers to aligning fuel standards across nations. Realizing this trajectory requires a coordinated global effort, including investment in port electrification and hydrogen supply chains, development and scaling of zero-carbon ship technologies, and intergovernmental alignment on emissions accounting frameworks. Without these enabling conditions, fragmented governance and technological inertia could delay the Net-Zero transition, risking irreversible Arctic ecosystem damage and undermining global climate goals.

As continued climate change increases the accessibility of the Arctic^{4,40,41}, the resulting shifts in maritime geography are poised to restructure global trade networks by redistributing economic opportunities and environmental burdens in profoundly unequal ways. Nations positioned to benefit from trans-Arctic shipping, such as Vietnam, South Korea, and Russia, may experience accelerated trade growth while other nations face marginalization as traditional routes lose strategic relevance. For example, the Suez Canal is currently a major source of foreign exchange for Egypt, contributing around 5% of the country's national GDP and generating over \$5 billion annually in toll fees, but it is economically exposed to traffic declines, with reduced flow directly diminishing canal revenues⁴². While trade forecasts may overstate the reliance on the ASR by neglecting intermodal alternatives such as trans-Eurasian rail, such unquantified local feedback as soot-induced sea ice loss suggests that our projections may underestimate the long-term regional impacts. Even under a Net-Zero scenario that eliminates carbon emissions, the non-carbon externalities of intensified Arctic traffic remain unaddressed. These externalities include increased underwater noise and the risk of ballast-mediated species invasions, oil spills, and ship strikes^{17,19,43,44}, all of which jeopardize the ecological integrity of polar marine systems. Realizing a sustainable maritime future requires harmonized global governance, including strengthened IMO enforcement, bilateral Arctic cooperation, and financing mechanisms for green technology deployment, integrated with biodiversity safeguards and community resilience to address the full spectrum of shipping impacts. Governance of the ASR must move beyond decarbonization to embrace a comprehensive environmental protection agenda^{22,24,45,46}, ensuring that economic gains do not come at the expense of irreversible harm to one of the planet's most climate-sensitive regions and aligning with United Nations Sustainable Development Goals for equitable global progress.

Methods

To quantify the carbon impact of access to the ASR, we developed the TISEP model, which integrates trade dynamics, vessel routing, and emissions data across climate and policy scenarios. The framework

consists of four interdependent modules: (1) forecasting trade volumes, (2) predicting global shipping flows, (3) the redistribution of Arctic shipping, and (4) estimating carbon emissions. Each module builds on the outputs of the previous one, forming a cohesive pipeline that captures how socioeconomic factors shape spatially resolved emissions across future scenarios (see Supplementary Fig. 11). First, we project the trade volumes between country pairs from 2025 to 2100 using an autoregressive integrated moving average with exogenous variables (ARIMAX) model trained on historical socioeconomic and geopolitical indicators such as GDP, population, transport cost, value-added structures, and bilateral political relations. We disaggregate these projections by vessel and commodity type under five SSPs. We select SSP2 as the baseline scenario for shipping flow projections in this study, as explained in the Supplementary Discussion. Next, we translate trade volumes into vessel flows across 150 national-level maritime routes, integrating AIS trajectory data with spatial route segmentation and flow reconstruction methods to derive route-specific vessel matrices aligned with trade projections. Third, we simulate the emergence of the ASR as a viable route by forecasting navigability based on sea ice conditions, estimating generalized transport costs, and identifying cost-optimal routing between country pairs. A trade reallocation model determines the usage of the ASR based on route competitiveness and seasonal accessibility, capturing shifts in the global shipping network. Lastly, we calculate shipping emissions using a hybrid bottom-up/top-down approach. We estimate historical emissions at the grid scale using AIS-derived vessel behavior and project future emissions by combining route-level traffic, energy demand, and scenario-specific fuel structures. The decarbonization trajectories include the BAU baseline, IMO-compliant regulation, green corridor strategies, and a net-zero transition. Together, these modules allow for a spatially explicit and scenario-resolved assessment of how Arctic accessibility and global trade growth will reshape maritime emissions through the 21st century. The following sections detail the computational procedures for each module.

Forecasting trade volumes

We employ a linear ARIMAX model to project bilateral trade volumes from 2025 to 2100 under the OTS and PTS. The modeling procedures, diagnostic tests, and forecast validation results are described in detail in Supplementary Method 1.

For the OTS, which serves as our baseline projection, is based on the assumption of a stable macroeconomic environment with gradually intensifying trade integration. The ARIMAX model integrates autoregressive and moving average terms alongside a wide array of explanatory variables including GDP, population, shared borders, language, legal agreements, and colonial ties⁴⁷. To capture contemporary trade dynamics, we incorporate two additional elements: (i) value-added trade links that reflect embedded economic relationships and (ii) transport cost heterogeneity as a frictional constraint. In addition, we capture geopolitical influence through bilateral political affinity (proxied by sentiments in joint news coverage) and interaction frequency (through co-mention rates in international media)^{48,49}. This scenario assumes no exogenous trade shocks and reflects a trajectory of uninterrupted trade normalization and structural growth. The ARIMAX model structure is

$$q_t^{OTS} = c + \sum_{i=1}^p \phi_i \ln q_{t-i} + \sum_{j=1}^q \theta_j \epsilon_{t-j} + \sum_{k=1}^q \beta_k \mathbf{X}_{kt} + \epsilon_t \quad (1)$$

where $\ln q_{t-i}$ and ϵ_{t-j} are autoregressive and moving average terms, respectively, and \mathbf{X}_{kt} denotes time-varying covariates capturing factors that influence trade flows between origin and destination countries (Supplementary Table 3). These factors include: (i) legal and institutional factors, e.g., `legal_new_o` and `legal_new_d` are dummies indicating the presence of recent bilateral or multilateral trade agreements for

origin and destination countries, and `fta_wto` captures World Trade Organization (WTO)-based free trade agreement status (binary); (ii) geopolitical and relational variables: `contig` indicates shared borders, `diplo_disagreement` measures logged diplomatic tension, and `intimacy` and `frequency` reflect the closeness and communication intensity of bilateral relations; and (iii) economic fundamentals: $\ln VA$ is the logarithm of value-added trade, $\ln Transport_cost_intensity$ denotes transport cost per unit trade, and $\ln gdp_i$, $\ln gdp_j$ and $\ln pop_i$, $\ln pop_j$ are the GDP and population logs of the origin and destination countries, respectively. The continuous predictors are log-transformed where appropriate. ϵ_t is the error term.

For the PTS, a recession-adjusted design is adopted to capture the uncertainty of future geopolitical and economic conditions such as trade wars, sanctions, and decoupling. This scenario builds on the OTS but imposes an initial global trade contraction in 2025 derived from WTO forecasts (https://www.wto.org/english/news_e/news25_e/tfore_16apr25_e.htm). The shock is modeled as a 0.2% decline in global trade volume. From 2026 to 2040, the system will recover along an exponentially decaying negative growth path parameterized with a 10-year half-life. This functional form captures the gradual diminution of the impact of the disruption while preserving continuity with the ARIMAX-projected long-term trend. Mathematically, the adjusted trade volume q_t^{PTS} is expressed as

$$q_t^{PTS} = q_{2024}^{OTS} \times \prod_{\tau=2025}^t (1 + g_{\tau}) \quad (2)$$

where $g_{\tau} = g_0 \times e^{-\lambda(\tau-2025)}$ for 2025–2040, with $\lambda = \ln(2)/10$, and $g_0 = -0.2\%$. After 2040, g_{τ} will revert to the baseline OTS growth rate. This hybrid formulation enables us to realistically account for short-term global trade shocks while preserving structural consistency in long-term forecasts.

Predicting global shipping flows

Building on our previous research⁵⁰, we refined the global shipping route network using Rodrigue’s maritime route map⁵¹. Since our trade predictions are at the national scale, the original shipping routes are segmented accordingly to ensure the accurate identification of vessel flows between the country pairs along these routes. This process identifies 150 national-level maritime routes for subsequent analysis (Supplementary Fig. 18). Based on the spatial distribution of maritime routes developed in this study, we construct buffer zones of varying sizes at the start and end points of each route. We determine the sizes and locations of these buffer zones by accounting for major strategic points such as the Cape of Good Hope and vessel operation patterns observed in AIS trajectory data. This approach, which our previous research validates, ensures the reliability of the vessel flow statistics along maritime routes. By integrating voyage information for six vessel types, we assign unique voyage IDs to each trajectory signal. Filtering of the AIS trajectory data within the buffer zones of each maritime route allows for the calculation of vessel flows along these routes using voyage IDs as

$$TF_{i,j,m} = \sum_m F_{n,p,q,i,j} \quad (3)$$

where $TF_{i,j,m}$ represents the total vessel flows along maritime route m between country i and country j . If vessel voyage n is simultaneously observed in buffer zones p and q of maritime route m , and the two countries involved in voyage n are i and j , then $F_{n,p,q,i,j} = 1$. By summing the flows of all of the vessels traveling between the countries i and j that appear in both buffer zones p and q , we are able to calculate the total vessel flows between this country pair along maritime route m .

Using AIS trajectory data from various ship types as input, we generate country-pair vessel flow matrices for the various ship types

across various shipping routes. This process involves analyzing 6.49 billion AIS trajectory data points in a Python 3.9 environment, resulting in 1494 country-pair vessel flow matrices, each sized 155×155 . We design the matrix dimensions to align with the size of the computed country trade matrix. Since the UN Commodity Trade Database does not provide separate trade volumes for general cargo, we combine the country-pair vessel flow matrices for general cargo and container ships to ensure a one-to-one correspondence between the trade and flow matrices. Utilizing the 155×155 country pair matrices of trade volumes from 2022, we map the total trade volumes of various categories between country pairs onto the corresponding 155×155 country-pair matrices of vessel flow. This mapping process generates trade-vessel flow matrices for various maritime routes. The mathematical formulation for this process is

$$TV_{i,j,k,m} = \frac{TF_{i,j,m}}{Trade_{i,j}} \quad (4)$$

where $TV_{i,j,k,m}$ denotes the ratio between vessel flows and trade volumes for commodity type k between country i and country j along maritime route m , $TF_{i,j,m}$ represents the total vessel flows along maritime route m between countries i and j , and $Trade_{i,j}$ indicates the trade volume between these two countries. For country pairs on certain maritime routes where neither trade volume nor vessel flow are observed, we assign the trade-vessel flow ratio a value of 0. Following the previous steps, we construct 1245 trade-vessel flow matrices for five commodity types, each with a size of 155×155 . These matrices represent the commodity categories of container, general cargo, bulk, oil, gas, and chemicals. By integrating the trade volume projections under the five SSPs, we can estimate the vessel flows between various country pairs along specific maritime routes as

$$Flow_{i,j,k,m} = PTrade_{i,j,k} \times TV_{i,j,k,m} \quad (5)$$

where $Flow_{i,j,k,m}$ represents the vessel flows for commodity type k between countries i and j on maritime route m , $PTrade_{i,j,k}$ refers to the projected trade volume between countries i and j under a specific SSP scenario, and $TV_{i,j,k,m}$ is calculated using Eq. (4). Subsequently, the total vessel flow along a specific maritime route can be determined as

$$Flow_{k,m} = \sum_{i,j} Flow_{i,j,k,m} \quad (6)$$

where $Flow_{k,m}$ is the vessel flow of commodity k on maritime route m . Lastly, we obtain the vessel flow projections for 150 maritime routes under the five SSP scenarios, with the time span of these projections aligning one-to-one with the trade projection results of the SSP scenarios. The results under the OTS are presented in Supplementary Figs. 19 and 20.

The redistribution of Arctic shipping

To estimate future trade flows through the ASR, we develop a cost-based routing framework incorporating (i) predictions of Arctic navigability, (ii) generalized shipping cost modeling and optimal route selection, and (iii) estimates of ASR trade allocation.

We project Arctic sea ice conditions, including sea ice thickness, sea ice concentration, and drift, from 2022 to 2100 under the SSP2 scenario. The methodology integrates the Coupled Model Intercomparison Project Phase 6 (CMIP6) climate projections with vessel-specific operability thresholds to determine navigable windows. Given the strong intra-annual variability of ice conditions, we generate forecasts at 10-day intervals (hereafter referred to as “periods”). Based on these projections, we delineate seasonally navigable corridors with and without the assistance of icebreakers across the 2022–2100

horizon⁵² (see Supplementary Figs. 21 and 22 for visual reference). The methodological details are in Supplementary Method 2.

Inspired by the OxMarTrans model⁵³, we develop a generalized shipping cost framework that incorporates Arctic navigation conditions. The generalized cost (GC) of transporting one ton of cargo from origin port i to destination port j is defined as the sum of monetary and time costs,

$$GC_{i,j,s,k} = \sum_{a \in A_{i,j}} \left(\frac{MC_{i,j,s,k,a}}{LF_{s,a}} + VOT_s \times T_{i,j,s,k,a} \right) \quad (7)$$

where GC denotes the generalized cost (USD ton⁻¹), MC is the monetary cost (USD ton⁻¹), VOT is the cargo’s value of time (USD ton⁻¹ h⁻²), T is total transport time (h), and LF is the load factor, accounting for the commercial utilization rate of the route. Subscripts i, j, s, k , and a refer to the origin, destination, vessel type, time period, and type of traversed area (Supplementary Table 4), respectively.

Transport time T can be expressed as the sum of transit time and transport delays (e.g., canal delays), and monetary costs, MC, are expressed as the sum of variable costs (which include distance- and time-related costs) and fixed costs:

$$T_{i,j,s,k,a} = \frac{Dis_{i,j,s,k,a}}{v_{s,a}} + Del_{i,j,s,k,a} \quad (8)$$

$$MC_{i,j,s,k,a} = DC_{i,j,s,k,a} + TC_{i,j,s,k,a} + Fix_{i,j,s,k,a} \quad (9)$$

where Dis represents the transport distance (in km), v is a vessel’s operational speed (km h⁻¹), Del is delay time (in hours), DC and TC are distance-related and time-related variable costs (USD ton⁻¹), respectively, and Fix denotes fixed charges (e.g., canal fees and icebreaking tariffs).

We further decompose the variable costs as

$$DC_{i,j,s,k,a} = (fc_{s,a} + ac_{s,a}) \times Dis_{i,j,s,k,a} \quad (10)$$

$$TC_{i,j,s,k,a} = \frac{Dis_{i,j,s,k,a}}{v_{s,a}} \times (Cap_{s,a} + Cre_{s,a} + Mai_{s,a} + Ins_{s,a}) \quad (11)$$

where fc and ac denote fuel and additional distance-related costs (USD ton⁻¹ km⁻¹), and Cap, Cre, Mai, and Ins represent the capital cost, crew cost, maintenance cost, and insurance cost per unit transport time (USD ton⁻¹ h⁻¹), respectively. The parameter values are detailed in the Supplementary Tables 5 and 6. Based on this generalized cost model, we develop a method to calculate optimal shipping routes and associated costs at a 1-degree grid scale (see Supplementary Method 3), thereby determining the least-cost paths between any two countries or regions.

We predict the annual trade ratio of Arctic shipping between countries (or regions) in the future based on the generalized cost determined through optimal path search. For each specific period k , we assume that vessels will choose the ASR if the cost is less than that of traditional routes (the maximum predicted cost between ports i and j for all periods). However, because of path dependency, political risks, and other difficult-to-quantify factors, cost-based predictions are likely to overestimate the actual Arctic shipping volume²⁶. To address this overestimation, we introduce a threshold, θ , to better capture these effects:

$$PA_{i,j,s,e} = \sum_{k \in K_e} (Y_{i,j,s,k} \times p_{s,k}) \quad (12)$$

$$Y_{i,j,s,k} = \begin{cases} 1, & \frac{GC_{i,j,s,k}}{\max\{GC_{i,j,s,k}|k \in K\}} < \theta_s \\ 0, & \frac{GC_{i,j,s,k}}{\max\{GC_{i,j,s,k}|k \in K\}} \geq \theta_s \end{cases} \quad \theta_s \in (0, 1) \quad (13)$$

where PA represents the trade ratio via ASR, p is the proportion of trade in a specific period relative to the total annual trade (used to account for seasonality, ignoring interannual differences), γ is a 0-1 variable, K is the set of all periods, e is the specific year, and θ is the critical threshold for vessels to choose the ASR determined by the actual values of the total transit volume along the Northern Sea Route for each ship type in 2024⁵⁴. The final Arctic trade ratio forecast data are provided in Supplementary Table 7.

Predicting shipping carbon emissions

Based on the 2022 AIS data (including vessel speed, position, and time) and vessel archive data (such as maximum rated power and design speed). We employ a bottom-up approach²⁷ to calculate carbon dioxide emissions at the trajectory scale³³. The calculation formula is

$$\begin{cases} E = E_m + E_a + E_b \\ E_m = P_m \times \left(\frac{V_{acc}}{V_{max}}\right)^3 \times T_v \times EF_m \\ E_a = P_{a,j} \times T_v \times EF_a \\ E_b = P_{b,j} \times T_v \times EF_b \end{cases} \quad (14)$$

where E represents a vessel's total emissions; E_m , E_a , and E_b represent emissions from the main engine (ME), auxiliary engine (AE), and boiler (BO), respectively; P_m , P_a , and P_b denote the rated power of the ME, AE, and BO, respectively; V_{acc} indicates the vessel's actual speed; V_{max} indicates the vessel's design speed; T_v represents the time that the vessel operates at speed V_{acc} ; the vessel's operational modes i (such as at berth, anchoring, maneuvering, and cruising) are defined by V_{acc} ; and EF_m , EF_a , and EF_b are the emission factors⁵⁵ for the ME, AE, and BO, respectively. The results are presented in Supplementary Fig. 25.

To explore long-term decarbonization pathways in maritime shipping, we construct one baseline scenario and three policy scenarios, each defined by distinct policy frameworks specifying emission targets, fuel mandates, and geographic coverage. These scenarios reflect a spectrum of ambition levels from inertial growth to full systemic decarbonization and are implemented within the TISEP model to quantify their respective impacts on global shipping emissions. The scenario-specific inputs include fuel mixes, policy timelines, and spatial applicability, all calibrated using historical AIS data, technological fuel forecasts, and institutional targets. The details of the scenarios are as follows.

BAU scenario. This baseline assumes that the global shipping sector maintains its exact 2025 fuel mix through 2100 with no further policy intervention, technological innovation, or behavioral shift. The fuel composition remains constant over time, consisting primarily of low-sulfur fuel oil (LSFO) and marine gas oil (MGO) (LSFO / MGO, 67.6%), HFO with scrubbers (17.7%), and liquefied natural gas (LNG) (12.5%), along with marginal shares of liquefied petroleum gas (0.4%), fossil methanol (0.4%), and bio-based marine gas oil (bio-MGO, 1.4%) (Supplementary Table 8). We assume that zero-carbon fuels (e.g., bio-LNG, e-fuels, and ammonia) and carbon capture technologies remain unused throughout the simulation period. Shipping demand continues to grow in line with projected trade flows, but the proportional composition of fuel use remains fixed at 2025 levels. As such, this scenario represents an inertial emissions trajectory under current operational and regulatory conditions and serves as the counterfactual

baseline for evaluating the mitigation potential of alternative pathways.

IMO 2023 strategy. This scenario assumes full compliance with the IMO's Revised GHG Strategy, which targets a 20% reduction in emissions by 2030, 70% by 2040, and net-zero by 2050 relative to 2008 levels¹². The scenario also envisions a progressive transition from fossil-based fuels to low- and zero-carbon alternatives, including methanol, ammonia, hydrogen, and e-fuels. The projected fuel mix is based on the Det Norske Veritas (DNV)'s predictive modeling, which incorporates fuel cost trajectories, technology readiness levels, and improvements in vessel energy efficiency. Specifically, the shares of HFO scrubbers and LSFO/MGO will decline from 17.7% and 67.6% in 2025 to 0% and 2.1% by 2050, respectively, while zero- and low-carbon fuels such as e-ammonia (27.6%), e-MGO (27.8%), and bio-methanol (2.9%) will become dominant (Supplementary Table 8). Carbon capture technologies will be progressively deployed from 2030 onward, accounting for a combined 40.8% of the fuel mix by 2050. This scenario reflects a policy-driven transformation of fuel structures aligned with mid-century decarbonization targets. Notably, the IMO's definition of "net-zero by or around 2050" refers to well-to-wake emissions, encompassing the entire fuel lifecycle, from production and transport to onboard combustion. This accounting framework allows fuels with upstream carbon mitigation (e.g., biofuels, e-ammonia with renewable electricity, or carbon capture at production sites) to qualify as zero-emission though combustion at sea still generates substantial tailpipe emissions. This distinction is particularly relevant for trans-Arctic shipping, during which vessels release residual CO₂ and black carbon directly into highly sensitive ecosystems. By contrast, the Net-Zero strategy introduced in this study involves the adoption of a stricter operational boundary, targeting zero emissions at the point of use (tank-to-wake) through the deployment of fully non-emitting technologies such as battery-electric systems, nuclear propulsion, and hydrogen fuel cells. This divergence highlights both the limitations of current international frameworks and the importance of spatially differentiated mitigation strategies for ecologically vulnerable regions.

The green corridor strategy. This strategy builds on the IMO pathway by introducing route-specific acceleration in green fuel adoption consistent with the Global Maritime Forum's strategy for green shipping corridors. Eight major corridors are designated as green corridors based on their ecological vulnerability and strategic significance (Supplementary Fig. 10). Within these corridors, the share of preferred green fuels such as LNG, methanol, and marine diesel oil will increase linearly from 2025 to 2050 to reach full substitution. For routes supporting multiple fuel options, the shares are evenly allocated. This scenario reflects both climate ambition and the operational challenges of low-carbon navigation in ice-prone and environmentally sensitive regions (Supplementary Table 9). Fuel selection varies by corridor depending on infrastructure readiness, trade function, and ecological risk. For example, e-ammonia is prioritized on iron ore routes such as South Africa–Europe and Western Australia–North Asia while bio-methanol and hydrogen are preferred along shorter, high-traffic corridors such as US–UK and Oslo–Rotterdam. The Green Corridor strategy is supported by the IMO and promoted through initiatives such as the Silk Alliance Green Corridor cluster. These efforts are grounded in the Clydebank Declaration launched at 26th United Nations Climate Change conference (COP26) and are implemented through multi-stakeholder collaborations involving port authorities, shipowners, financial institutions, and fuel providers. Notably, the ASR is incorporated as a green corridor in this study because of its projected strategic importance and environmental sensitivity. Although it is not featured in current policy frameworks, its inclusion here reflects the need to extend decarbonization efforts to emerging high-latitude routes. Given the ecological fragility of the Arctic, high-risk fuels such

as ammonia are excluded, and lower-impact options, including carbon capture and storage (CCS)-equipped LSFO, CCS LNG, and methanol, are substituted to minimize environmental harm.

The net-zero strategy. This scenario represents a high-ambition pathway toward decarbonization of the maritime sector, surpassing existing strategies such as those laid out by the IMO 2023 strategy and the Green Corridor initiatives. The scenario assumes the phased adoption of zero-carbon energy carriers—specifically, electricity, hydrogen, and nuclear—beginning regionally in the Arctic in 2040 and expanding globally from 2050 onward. The earlier regional deployment reflects the Arctic’s environmental sensitivity and the amplified climate feedback driven by black carbon and CO₂ emissions. The urgent need to mitigate accelerated warming in this region, exacerbated by growing trans-Arctic shipping activity, justifies its prioritization for a zero-emission transition. Under this scenario, zero-carbon fuels will remain negligible prior to 2045, when their initial deployment will begin exclusively in the Arctic. By 2050, global-scale adoption will commence, supported by anticipated infrastructure development, carbon pricing mechanisms, and regulatory enforcement. Between 2045 and 2100, the share of zero-carbon energy share in total maritime energy use will increase exponentially, from 0.14% in 2045 to 39.6% in 2055, and 86.6% in 2070, reaching 100% by 2100. This trajectory captures the expected curve of technology diffusion, regulatory maturation, and the system-wide substitution of fossil-based marine fuels (Supplementary Fig. 26). Real-world initiatives such as Green Shipping Corridors are assumed to serve as early pilot projects for zero-emission deployment, particularly in technologically advanced ports. The Net-Zero strategy thus defines the upper bound of maritime decarbonization potential and assumes the complete and irreversible transition to non-emitting propulsion technologies across all vessel classes and regions by the end of the century.

Projecting short-term carbon emissions (2025–2050). Because of the absence of well-established emission factors for many clean fuels in bottom-up models, we adopt a hybrid approach that integrates both bottom-up and top-down methods to project future shipping emissions. We begin by estimating energy consumption at the vessel-trajectory level using data on engine power, operational speed, and voyage duration. We aggregate these values by route and vessel type to derive the baseline energy demand for each category. Unit energy consumption per vessel is then calculated and scaled by projected traffic flows to estimate total annual energy demand through 2100. Next, we determine the required fuel mass by combining the projected energy demand with the mass share and specific fuel consumption of each fuel type, the latter being defined as the fuel mass required to produce one unit of energy. Lastly, we calculate carbon emissions by multiplying the annual fuel mass of each type by its corresponding emission factor. The full calculation procedure is

$$\begin{cases} W_{c,t,y_0} = \sum_{j \in J} J_{c,t} \left[P_m \times \left(\frac{V_{act,j}}{V_{max}} \right)^3 \times T_{v,j} + P_c \times T_{v,j} + P_b \times T_{v,j} \right] \\ W_{c,t,y} = \left(\frac{W_{c,t,y_0}}{N_{c,t,y_0}} \right) \times N_{c,t,y} \\ W_{c,t,y} = \sum_i \left(M_{c,t,y} \times \frac{r_{i,c,t,y}}{SFC_i} \right) \\ E_{c,t,y} = \sum_i \left(M_{c,t,y} \times r_{i,c,t,y} \times EF_i \right) \end{cases} \quad (15)$$

where y_0 denotes the baseline year 2022 in this study, W_{c,t,y_0} is the baseline energy consumption for route c and ship type t , N_{c,t,y_0} is the number of ships in the baseline year, $N_{c,t,y}$ is the projected ship volume for year y , $r_{i,c,t,y}$ is the mass-based fuel share of fuel type i , SFC_i is the specific fuel consumption of fuel type i (see Supplementary Table 10), EF_i is the emission factor of fuel type i (see Supplementary Table 11), and $E_{c,t,y}$ represents the total carbon emissions.

Projecting long-term carbon emissions (2050–2100). For the long-term projection from 2050 to 2100, we employ two distinct approaches depending on the policy scenario. Under the IMO and Green Corridor strategies, we extrapolate emissions based on the historical trend of the Energy Efficiency Operational Indicator (EEOI) from 2025 to 2050. We apply a log-linear regression model to EEOI values by route and ship type to estimate future emission intensities. The EEOI is defined as

$$EEOI_{r,t,y} = \frac{E_{r,t,y}}{N_{r,t,y} \times d_r} \quad (16)$$

where $E_{r,t,y}$ is the total carbon emissions for route r , ship type t , and year y ; $N_{r,t,y}$ is the number of voyages; and d_r is the distance of route r . Under the Net-Zero strategy, zero-carbon fuel uptake is modeled as an exponential growth process beginning in 2040 for Arctic routes and in 2050 for all other global routes. The residual share of conventional fuels follows the 2050 Green Corridor fuel structure and declines exponentially over time. We calculate emissions using the same method as Eq. (15). The share of conventional fuels, defined as the complement to zero-carbon penetration, is

$$W_{r,t,y}^{conv} = e^{-k(y-y_0)} \times W_{r,t,y} \quad (17)$$

where y_0 is the implementation start year and k is a scaling factor set to ensure that zero-carbon energy reaches full adoption by 2100.

Data availability

The study-generated datasets that support the findings of this work have been deposited in Zenodo (<https://doi.org/10.5281/zenodo.14550743>). Source data for all figures are provided with the paper and the accompanying code. Access to the AIS data is restricted for third parties, so we use the data under license for the current study. The Harmonized System (HS) code is based on the HS22 standard, and the relationship between ship types and HS codes can be accessed in the Fourth IMO GHG Study. The trade volume data are from CEPII BACI (https://www.cepii.fr/CEPII/en/bdd_modele/bdd_modele_item.asp?id=37). The seaborne proportion is from <https://unctadstat.unctad.org/datacentre/dataviewer/US.SeaborneTrade>. The transport cost is from <https://unctadstat.unctad.org/EN/TransportCost.html> (accessed on 17 July 2024), ranging from 2016 to 2021. The GDP and population data included historical data (for 1995–2022) and prediction data (for 2100), which we obtain from the World Bank Databank (<http://databank.worldbank.org/>, accessed on 17 July 2024) and the International Institute for Applied Systems Analysis’s shared socioeconomic pathway (SSP) database (<https://tntcat.iiasa.ac.at/SspDb/>, accessed on 17 July 2024), respectively. We obtain the Global Database of Events, Language, and Tone (GDELT) data from the GDELT Project (<https://www.gdelproject.org/>). We simulate the forecasted GDP and population data based on various shared socioeconomic pathways. The value-added data are from the Eora Global Supply Chain Database (<https://worldmrio.com/>). The bilateral maritime distances are from the Foundation for Studies and Research on International Development (<https://zenodo.org/record/46822#.VvFcNWMvjjp>). The sea area data are from Marinerregions.org (<https://www.marinerregions.org/downloads.php>). Source data are provided with this paper.

Code availability

The Python codes used during the current study are available from Zenodo (<https://doi.org/10.5281/zenodo.14550743>).

References

- Notz, D. & SIMIP Community. Arctic sea ice in CMIP6. *Geophys. Res. Lett.* **47**, e2019GL086749 (2020).
- Stroeve, J. & Notz, D. Changing state of Arctic sea ice across all seasons. *Environ. Res. Lett.* **13**, 103001 (2018).

3. Aksenov, Y. et al. On the future navigability of Arctic sea routes: High-resolution projections of the Arctic Ocean and sea ice. *Mar. Policy* **75**, 300–317 (2017).
4. Mudryk, L. R. et al. Impact of 1, 2 and 4°C of global warming on ship navigation in the Canadian Arctic. *Nat. Clim. Change* **11**, 673–679 (2021).
5. Schøyen, H. & Bråthen, S. The Northern Sea Route versus the Suez Canal: cases from bulk shipping. *J. Transp. Geogr.* **19**, 977–983 (2011).
6. Li, Z. et al. Cost-benefit analysis of a trans-Arctic alternative route to the Suez Canal: a method based on high-fidelity ship performance, weather, and ice forecast models. *J. Mar. Sci. Eng.* **11**, 711 (2023).
7. Bekkers, E., Francois, J. F. & Rojas-Romagosa, H. Melting ice caps and the economic impact of opening the Northern Sea Route. *Econ. J.* **128**, 1095–1127 (2018).
8. Corbett, J. J. et al. Arctic shipping emissions inventories and future scenarios. *Atmos. Chem. Phys.* **10**, 9689–9704 (2010).
9. Intergovernmental Panel on Climate Change. *Climate Change 2022: Mitigation of Climate Change. Contribution of Working Group III to the Sixth Assessment Report of the Intergovernmental Panel on Climate Change* (Cambridge University Press, Cambridge, UK, 2022).
10. Rodríguez, J. P. et al. Shipping traffic through the Arctic Ocean: spatial distribution, temporal evolution and its dependence on the sea ice extent. *J. Mar. Syst.* **256**, 107500 (2024).
11. Dalsøren, S. B. et al. Environmental impacts of shipping in 2030 with a particular focus on the Arctic region. *Atmos. Chem. Phys.* **13**, 1941–1955 (2013).
12. International Maritime Organization. *2023 IMO Strategy on Reduction of GHG Emissions from Ships*. IMO Doc. MEPC 80/Res. MEPC.377(80). International Maritime Organization (2023).
13. Cristea, A. et al. Trade and the greenhouse gas emissions from international freight transport. *J. Environ. Econ. Manag.* **65**, 153–173 (2013).
14. Deng, S. & Mi, Z. A review on carbon emissions of global shipping. *Mar. Dev.* **1**, 4 (2023).
15. Chen, J. et al. Projected emissions and climate impacts of Arctic shipping along the Northern Sea Route. *Environ. Pollut.* **341**, 122848 (2024).
16. Yumashev, D. et al. Towards a balanced view of Arctic shipping: estimating economic impacts of emissions from increased traffic on the Northern Sea Route. *Clim. Change* **143**, 143–155 (2017).
17. Johansson, L., Jalkanen, J.-P. & Kukkonen, J. Global assessment of shipping emissions in 2015 on a high spatial and temporal resolution. *Atmos. Environ.* **167**, 403–415 (2017).
18. Svavarsson, J. et al. Pollutants from shipping—new environmental challenges in the subarctic and the Arctic Ocean. *Mar. Pollut. Bull.* **164**, 112004 (2021).
19. Afenyo, M., Jiang, C. & Ng, A. K. Y. Climate change and Arctic shipping: A method for assessing the impacts of oil spills in the Arctic. *Transp. Res. Part D* **77**, 476–490 (2019).
20. Osipova, L. & Gore, K. *Black Carbon and CO₂ Emissions from EU Regulated Shipping in the Arctic* (International Council on Clean Transportation, 2025).
21. Chen, Y. & Cheng, K. Decarbonizing Arctic shipping: governance pathways and future directions. *Front. Mar. Sci.* **12**, 1489091 (2025).
22. International Maritime Organization. *International Code for Ships Operating in Polar Waters (Polar Code)*. <https://www.imo.org/en/ourwork/safety/pages/polar-code.aspx> (2015).
23. Arctic Council. *Arctic Shipping Status Report #3: Heavy Fuel Oil Use in the Arctic*. <https://oarchive.arctic-council.org/server/api/core/bitstreams/9b7ee1fc-3649-4be9-a4ac-a641d4171292/content> (2021).
24. Young, O. R. & Kim, J. D. Next steps in Arctic Ocean governance: meeting the challenge of coordinating a dynamic regime complex. *Mar. Policy* **133**, 104726 (2021).
25. Jing, D. et al. CO₂ emission projection for Arctic shipping: a system dynamics approach. *Ocean Coast. Manag.* **205**, 105531 (2021).
26. Zhang, Y., Meng, Q. & Ng, S. H. Shipping efficiency comparison between Northern Sea Route and the conventional Asia-Europe shipping route via Suez Canal. *J. Transp. Geogr.* **57**, 241–249 (2016).
27. Wang, X. T. et al. Trade-linked shipping CO₂ emissions. *Nat. Clim. Change* **11**, 945–951 (2021).
28. Aalto, P., Hanhijärvi, M. & Narita, D. Short- and long-term solutions for mitigating black carbon emissions in Arctic shipping: Implications for stakeholders. *Mar. Policy* **173**, 106565 (2025).
29. Shu, Y., Cui, H. & Song, L. Influence of sea ice on ship routes and speed along the Arctic Northeast Passage. *Ocean Coast. Manag.* **256**, 107320 (2024).
30. Kramel, D. et al. Advancing SSP-aligned scenarios of shipping toward 2050. *Sci. Rep.* **14**, 8965 (2024).
31. Silk Alliance. *The Silk Alliance: Fleet decarbonisation strategy for green corridor implementation* (LR Maritime Decarbonisation Hub, 2022).
32. DNV. *Key Considerations for Establishing a Green Shipping Corridor* DNV (2022). <https://www.dnv.com/expert-story/maritime-impact/key-considerations-for-establishing-a-green-shiping-corridor/#:~:text=In%20step%201%20of%20DNV's,financial%20tools%20and%20support%20mechanisms>. Accessed 23 Sept 2025.
33. Comer, B. & Osipova, L. *Accounting for Well-to-Wake Carbon Dioxide Equivalent Emissions in Maritime Transportation Climate Policies* (International Council on Clean Transportation, 2021).
34. DNV. *Maritime Forecast to 2050: A Deep Dive into Shipping's Decarbonization Journey*. *Energy Transition Outlook 2024*. <https://www.dnv.com/maritime/maritime-forecast/> (2024).
35. Zhou, Z. & Tao, J. Hydrogen-powered vessels in green maritime decarbonization: policy drivers, technological frontiers and challenges. *Front. Mar. Sci.* **12**, 1601617 (2025).
36. Wang, Q., Zhang, H. & Zhu, P. Using nuclear energy for maritime decarbonization and related environmental challenges: existing regulatory shortcomings and improvements. *Int. J. Environ. Res. Public Health* **20**, 2993 (2023).
37. Cariou, P., Parola, F. & Notteboom, T. Towards low carbon global supply chains: a multi-trade analysis of CO₂ emission reductions in container shipping. *Int. J. Prod. Econ.* **208**, 17–28 (2019).
38. Johannessen, O. M. & Miles, M. W. Critical vulnerabilities of marine and sea ice-based ecosystems in the high Arctic. *Reg. Environ. Change* **11**, 239–248 (2011).
39. Boertmann, D. & Mosbech, A. *Eastern Baffin Bay—A Strategic Environmental Impact Assessment of Hydrocarbon Activities*. Danish Centre for Environment and Energy Report No. 19 (Aarhus University Press, Aarhus, Denmark, 2011).
40. Rodríguez, J. P. et al. Shipping traffic through the Arctic Ocean: spatial distribution, seasonal variation and its dependence on the sea ice extent. *iScience* **27**, 110236 (2024).
41. Stephenson, S. R., Smith, L. C. & Agnew, J. A. Divergent long-term trajectories of human access to the Arctic. *Nat. Clim. Change* **1**, 156–160 (2011).
42. Kenawy, E. The economic impacts of the new Suez Canal. *IEMed Mediterranean Yearbook*, 282–288 (European Institute of the Mediterranean, 2016).
43. Khan, B., Khan, F. & Veitch, B. A dynamic Bayesian network model for ship-ice collision risk in the Arctic waters. *Saf. Sci.* **130**, 104858 (2020).
44. Rosenhaim, I. L. et al. Simulated ballast water accumulation along Arctic shipping routes. *Mar. Policy* **103**, 9–18 (2019).
45. Huntington, H. P. et al. Effects of Arctic commercial shipping on environments and communities: context, governance, priorities. *Transp. Res. Part D* **118**, 103731 (2023).

46. Dalaklis, D. et al. Future Arctic regulatory interventions: Discussing the impact of banning the use of heavy fuel oil. *Polar Geogr.* **46**, 75–94 (2023).
 47. Kabir, M., Salim, R. & Al-Mawali, N. The gravity model and trade flows: Recent developments in econometric modeling and empirical evidence. *Econ. Anal. Policy* **56**, 60–71 (2017).
 48. Macis, L. et al. Breaking the trend: anomaly detection models for early warning of socio-political unrest. *Technol. Forecast. Soc. Change* **206**, 123495 (2024).
 49. Van Haren, J. *International Trade and Sentiment: To What Extent do they Predict Each Other*. Master's thesis. <https://www.tilburguniversity.edu> (2020).
 50. He, Z. et al. Analyzing foreland dynamics in China's port clusters under global major events (2019–2022) by AIS trajectory data. *Ocean Coast. Manag.* **255**, 107269 (2024).
 51. Rodrigue, J.-P. Maritime transport. in *International Encyclopedia of Geography: People, the Earth, Environment and Technology* (eds Richardson, D. et al.) 1–7 (Wiley-Blackwell, Hoboken, NJ, 2017).
 52. Zhao, P., Li, Y. & Zhang, Y. Ships are projected to navigate year-round along the North Sea Route by 2100. *Commun. Earth Environ.* **5**, 407 (2024).
 53. Verschuur, J., Koks, E. E. & Hall, J. W. Ports' criticality in international trade and global supply-chains. *Nat. Commun.* **13**, 4351 (2022).
 54. Main results of NSR transit navigation in 2024. *Centre for High North Logistics*. <https://chnl.no/news/main-results-of-nsr-transit-navigation-in-2024/> (2024).
 55. Liu, H., Fu, M. & Jin, X. Health and climate impacts of ocean-going vessels in East Asia. *Nat. Clim. Change* **6**, 1037–1041 (2016).
- redistribution. S.Z. processed the AIS data and contributed to figure production. W.K. participated in data processing.

Competing interests

The authors declare no competing interests.

Additional information

Supplementary information The online version contains supplementary material available at <https://doi.org/10.1038/s41467-025-64437-4>.

Correspondence and requests for materials should be addressed to Pengjun Zhao or Caixia Zhang.

Peer review information *Nature Communications* thanks Alexander Chupin, and the other anonymous, reviewer(s) for their contribution to the peer review of this work. A peer review file is available.

Reprints and permissions information is available at <http://www.nature.com/reprints>

Publisher's note Springer Nature remains neutral with regard to jurisdictional claims in published maps and institutional affiliations.

Open Access This article is licensed under a Creative Commons Attribution-NonCommercial-NoDerivatives 4.0 International License, which permits any non-commercial use, sharing, distribution and reproduction in any medium or format, as long as you give appropriate credit to the original author(s) and the source, provide a link to the Creative Commons licence, and indicate if you modified the licensed material. You do not have permission under this licence to share adapted material derived from this article or parts of it. The images or other third party material in this article are included in the article's Creative Commons licence, unless indicated otherwise in a credit line to the material. If material is not included in the article's Creative Commons licence and your intended use is not permitted by statutory regulation or exceeds the permitted use, you will need to obtain permission directly from the copyright holder. To view a copy of this licence, visit <http://creativecommons.org/licenses/by-nc-nd/4.0/>.

© The Author(s) 2025

Acknowledgements

The research is funded by the National Natural Science Foundation of China: 42525101(P.Z.); 42130402 (P.Z.); 42506237(C.Z.).

Author contributions

P.Z. led the development of the research plan, conceptualized the research questions, and led the manuscript writing. Y.L. developed the core modeling framework, processed the data, and generated the figures. C.Z. contributed to the formulation of research questions and co-lead the manuscript writing. T.K., X.Z., and Y.X. performed the global shipping carbon-emissions calculations. Z.H. and G.H. conducted the global shipping flow analysis and led the modeling of Arctic shipping